Article

Cell Reports

Augmentation of Myc-Dependent Mitotic Gene Expression by the Pygopus2 Chromatin Effector

Graphical Abstract

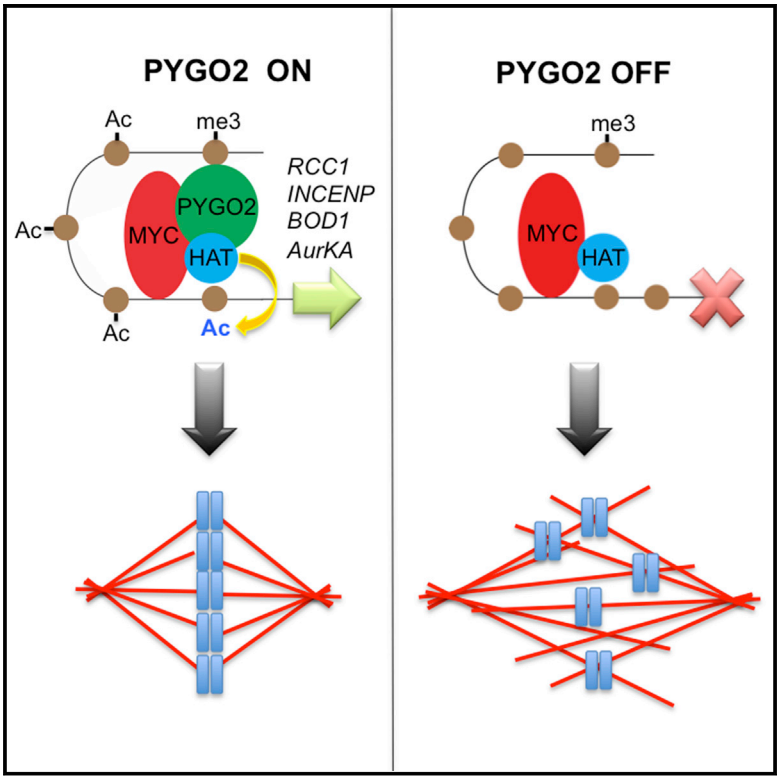

Authors

Phillip G.P. Andrews, Catherine Popadiuk, Thomas J. Belbin, Kenneth R. Kao

Correspondence

kkao@mun.ca

In Brief

Pygo2 is emerging as a key chromatin effector in a variety of human cancers. Distinct from its role in the active Wnt/β-catenin transcriptional complex, Andrews et al. identify Pygo2 as a critical component of oncogenic MYC transcriptional complexes that control mitotic gene expression.

Highlights

- Loss of Pygo2 in cancer cells disrupts chromosome congression
- Pygo2 interacts with the MYC oncoprotein
- MYC and Pygo2 associate with a common set of growth-related genes
- MYC depends on Pygo2 to activate biorientation and segregation genes

Data and Software Availability

GSE112291

Andrews et al., 2018, Cell Reports *23*, 1516–1529
May 1, 2018
https://doi.org/10.1016/j.celrep.2018.04.020

CellPress

OPEN ACCESS
CellPress

Cell Reports
Article

Augmentation of Myc-Dependent Mitotic Gene Expression by the Pygopus2 Chromatin Effector

Phillip G.P. Andrews,[1] Catherine Popadiuk,[2] Thomas J. Belbin,[3] and Kenneth R. Kao[1,3,4,*]
[1]Terry Fox Cancer Research Labs, Division of Biomedical Sciences, Faculty of Medicine, Memorial University, St. John's Campus, NL A1B 3V6, Canada
[2]Division of Gynecologic Oncology, Faculty of Medicine, Memorial University, St. John's Campus, NL A1B 3V6, Canada
[3]Discipline of Oncology, Faculty of Medicine, Memorial University, St. John's Campus, NL A1B 3V6, Canada
[4]Lead Contact
*Correspondence: kkao@mun.ca
https://doi.org/10.1016/j.celrep.2018.04.020

SUMMARY

Mitotic segregation of chromosomes requires precise coordination of many factors, yet evidence is lacking as to how genes encoding these elements are transcriptionally controlled. Here, we found that the Pygopus (Pygo)2 chromatin effector is indispensable for expression of the MYC-dependent genes that regulate cancer cell division. Depletion of Pygo2 arrested SKOV-3 cells at metaphase, which resulted from the failure of chromosomes to capture spindle microtubules, a critical step for chromosomal biorientation and segregation. This observation was consistent with global chromatin association findings in HeLa S3 cells, revealing the enrichment of Pygo2 and MYC at promoters of biorientation and segmentation genes, at which Pygo2 maintained histone H3K27 acetylation. Immunoprecipitation and proximity ligation assays demonstrated MYC and Pygo2 interacting in nuclei, corroborated in a heterologous MYC-driven prostate cancer model that was distinct from Wnt/β-catenin signaling. Our evidence supports a role for Pygo2 as an essential component of MYC oncogenic activity required for mitosis.

INTRODUCTION

Chromosomal biorientation, required for segregation, occurs by a search-and-capture mechanism whereby spindle microtubules emanating from the centrosomes attach to sister kinetochores (Foley and Kapoor, 2013; Tanaka, 2013, 2010; Tanenbaum and Medema, 2010). This mechanism relies on the Knl-1/MIS12/NDC80 (KMN) network, which facilitates physical contacts between spindle microtubules and centromeric DNA (Varma and Salmon, 2012). In addition to search and capture, other mechanisms exist to efficiently drive biorientation. For example, the kinetochore protein TPX2 associates with nucleating microtubules that aid in spindle-kinetochore capture (Katayama et al., 2008). Another major driver of microtubule-kinetochore interaction and capture is the Regulator of Chromosome Condensation 1 (RCC1)-mediated RanGTP concentration gradient that exists around mitotic chromosomes to promote microtubule nucleation (Kalab and Heald, 2008). Moreover, several families of serine-threonine kinases, including the Aurora Kinases (AurKs) and the Polo-like kinases (Plks), are required for mitosis and have documented roles in cancer (Degenhardt and Lampkin, 2010; Goldenson and Crispino, 2015). The AurKs and Plks are associated with many key mitotic events, such as mitotic entry, centrosome and kinetochore maturation, kinetochore-microtubule attachment, spindle assembly, and cytokinesis (Archambault et al., 2015; Carmena et al., 2009, 2012).

How large sets of genes responsible for mitosis are transcriptionally regulated is a question of biological importance for which evidence is lacking. One key factor is MYC, a transcriptional master regulator of stem cell fate (Fagnocchi and Zippo, 2017) and cancer cell growth (Dang, 2012, 2013). MYC is a basic helix-loop-helix leucine zipper protein that heterodimerizes with its partner MAX and associates with E-box elements in promoter regions of genes leading to transcriptional activation (Blackwood and Eisenman, 1991). MYC is associated with the enhancers/promoters of most active genes in malignant cells, with the overall outcome of aberrant MYC expression being transcriptional amplification that drives tumor growth (Lin et al., 2012; Nie et al., 2012). MYC activates the expression of essential mitotic genes, including RCC1 and AurKA/B (den Hollander et al., 2010; Tsuneoka et al., 1997), and plays multiple roles during mitosis to ensure cell division and mitotic cell fate (Annibali et al., 2014; Topham et al., 2015). Understanding MYC regulation and function, consequently, has been a major focus in tumor biology research (Dang et al., 2017; Meyer and Penn, 2008; Whitfield et al., 2017).

In this study, we present evidence supporting a requirement of the Pygopus (Pygo) protein for MYC-dependent activation of mitosis-related genes. Pygo was originally described as a dedicated component of the Wnt/β-catenin transcription complex (Kramps et al., 2002; Parker et al., 2002; Thompson et al., 2002), with two Pygo orthologs in mammalian cells. Pygo1 is dispensable for normal murine development (Schwab et al., 2007), and its potential role in cancer is not yet identified. Pygo2, on the other hand, is of interest, given its elevated expression and utilization for malignant growth in a number of different cancers (Andrews et al., 2007; Liu et al., 2013; Popadiuk et al., 2006; Zhang et al., 2015; Kao et al., 2017). At actively transcribing

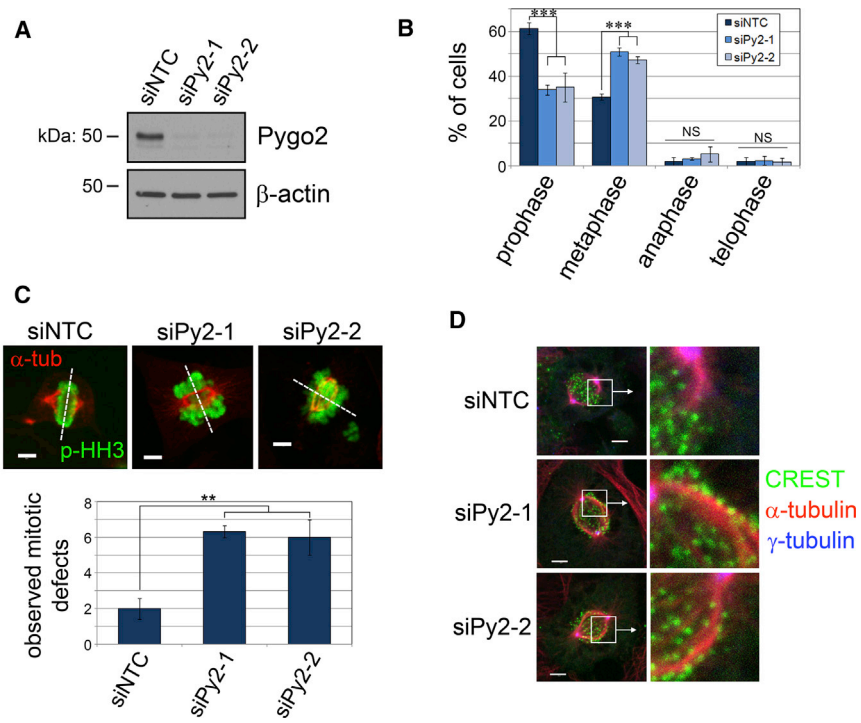

Figure 1. Pygo2 Depletion Disrupts Spindle-Kinetochore Alignment in Early Metaphase Cells

(A) Immunoblots demonstrate a reduction of Pygo2 protein in SKOV-3 cells that were treated with a non-targeting siRNA (siNTC) or two Pygo2-specific siRNAs (siPy2-1 and siPy2-2); β-actin was used to as a loading control.

(B) Pygo2-depleted SKOV-3 cells co-stained with α-tubulin and phospho-histone H3 (p-HH3). Pygo2-depleted cells resulted in a significant accumulation of cells in metaphase, consistent with a mitotic delay (***$p < 0.001$; NS, not significant).

(C) Top panel: confocal images of SKOV-3 cells co-stained with α-tubulin and p-HH3 (scale bars, 5 μm). Bottom panel: quantification of observed mitotic defects, showing an increased number of defects in Pygo2-depleted SKOV-3 cells (**$p < 0.01$).

(D) Confocal images of Pygo2-depleted SKOV-3 cells at early metaphase co-stained with anti-centromere antisera CREST (centromeres) and α-tubulin (spindle) and γ-tubulin (spindle poles) (scale bar, 5 μm).

Bar graphs represent averages ± SEM. See also Figure S1.

genes, Pygo2 binds specific histone marks of activation such as H3K4me3, where it recruits histone acetyltransferase (HAT) activity, which promotes an open euchromatic structure (Andrews et al., 2009; Chen et al., 2010; Fiedler et al., 2008). In cancer, Pygo2 participates in the expression of highly transcribed RNAs essential for DNA replication and cell-cycle progression (Andrews et al., 2013; Gu et al., 2012). These observations raised the possibility that Pygo2 acts epigenetically as a transcriptional "euchromatic switch" in deregulated cell growth and division, such as in mammary tumor initiation (Watanabe et al., 2014).

We identified an interaction between Pygo2 and MYC and, through genome-wide analysis, discovered that they were associated with a common subset of genes that facilitate chromosome biorientation and segregation. While independent of canonical Wnt signaling, the established function of Pygo2 as a critical chromatin effector was corroborated by its ability to maintain acetylation of H3K27 at the enhancers/promoters of key MYC-target genes that promote interactions between chromosomes and spindle microtubules. Thus, in addition to its role in Wnt/β-catenin signaling, Pygo2 acts as an epigenetic accessory protein, utilized in a MYC-dependent transcriptional program controlling genes critical for cell division.

RESULTS

Pygo2 Depletion Disrupts Spindle-Kinetochore Recognition and Chromosome Biorientation

Deprivation of Pygo2 in the p53 null SKOV-3 epithelial ovarian cancer cell line caused cell-cycle arrest (Popadiuk et al., 2006), with an accumulation of cells in G2/M (Andrews et al., 2013). Similar G2/M accumulations resulting from Pygo2 depletion were found in several other p53 null cell lines, including PC3 prostate cancer cells (Figure S1A). To examine the possible role of Pygo2 in cell division, we compared the mitotic profiles of SKOV-3 cells treated with two small interfering RNAs (siRNAs) targeting Pygo2 (siPy2-1 and siPy2-2; Figures 1A and S1B), along with a non-targeting siRNA control (siNTC).

Immunofluorescent staining, using anti phospho-histone H3 (p-HH3) and α-tubulin antibodies to mark mitotic cells, revealed that Pygo2 depletion significantly increased the proportion of metaphase cells with a corresponding decrease of cells in prophase (Figure 1B). Moreover, Pygo2-depleted cells displayed defects in which mitotic spindles appeared abnormal and the chromosomes failed to line up at metaphase plates (Figure 1C). It appeared that the chromosomes were not efficiently captured by spindle microtubules, resulting in chromosome biorientation defects.

To exclude the possibility of defective mitotic spindle microtubules, cells were stained for α- and γ-tubulin, which are localized at the centrosomes and are required for microtubule nucleation (Kollman et al., 2011). In Pygo2-depleted cells, γ-tubulin was largely unaffected, compared to the control-treated cells. The spindle microtubules, however, were abnormally long and coincided with misaligned chromosomes (Figure S1C). While there was no change in the centrosomal localization of AurKA or active, phosphorylated AurKA (P-T288), an overall decrease in staining intensity was observed in both AurKA and AurKA P-T288 in Pygo2-depleted cells (Figure S1D).

To examine chromosome capture, we assessed the localization of spindle microtubules with respect to centromeres using α-tubulin and anti-centromere (CREST) antibodies (Figure 1D). In Pygo2-depleted cells, spindle microtubules failed to align

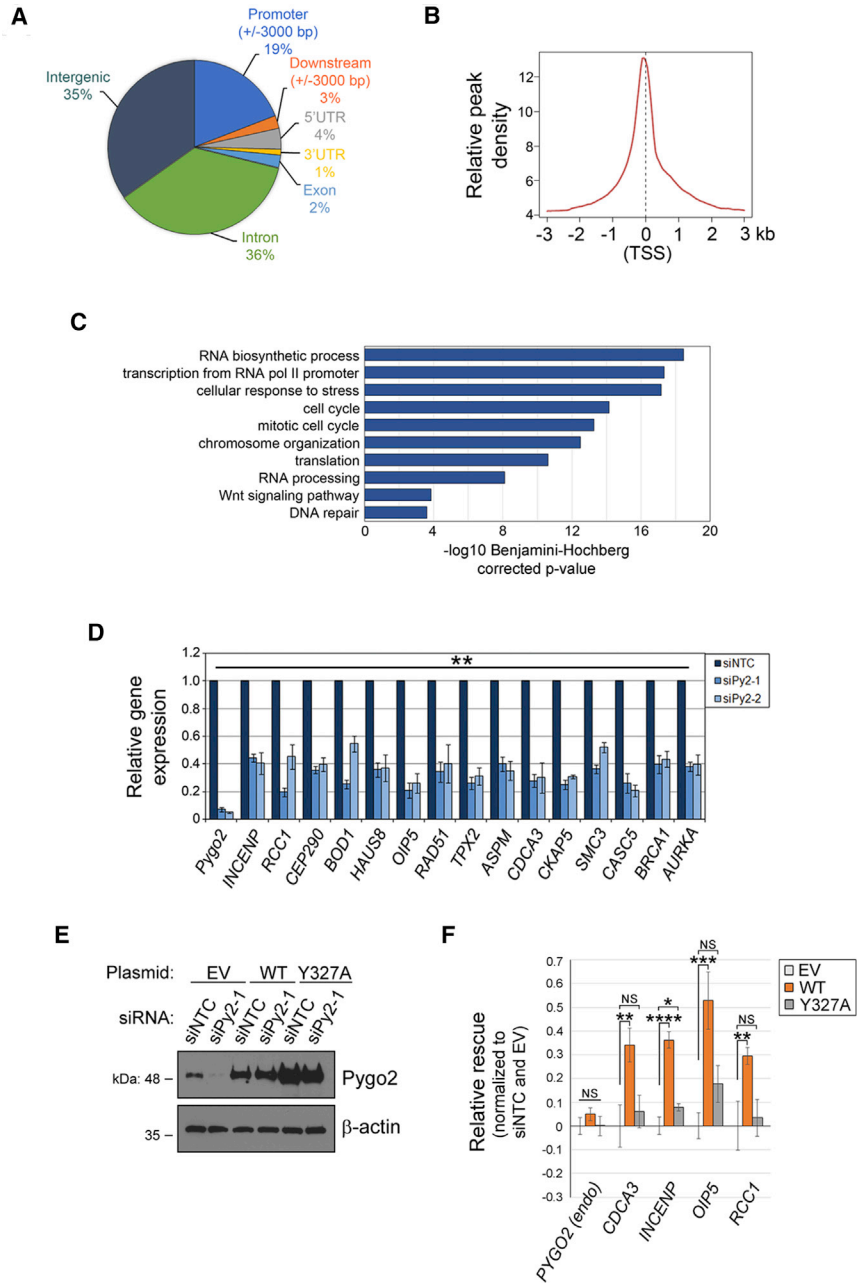

Figure 2. Pygo2 Is Essential for Mitotic Gene Expression

(A) Genomic distribution of significant Pygo2 ChIP-seq peaks.

(B) Average binding profile of Pygo2 at TSS (±3 kb).

(C) Functional enrichment analysis of biological processes associated with Pygo2 ChIP-seq genes (TSS ±2 kb). Note enrichment of genes involved in cell cycle and mitosis (marked with an asterisk).

(D) Depletion of Pygo2 in HeLa S3 cells followed by qRT-PCR validates RNA expression of Pygo2 and 15 candidate Pygo2 target genes with ascribed function in chromosome biorientation and cell division.

(E) HeLa S3 cells were treated with control siRNAs (siNTC) or Pygo2 3′ UTR-specific siRNAs (siPy2-1). Co-transfected rescuing plasmids include empty pCS2 plasmid (EV), pCS2-Pygo2 WT coding region (WT), or pCS2-Pygo2 Y327A (H3K4me3 binding mutant; Y327A). Immunoblots were performed to assess the relative expression of Pygo2 (exogenous + endogenous); β-actin was used as a loading control.

(F) qRT-PCR analysis was performed to assess the relative rescuing ability of Pygo2 (WT) and Pygo2 Y327A (Y327A) on select cell division genes (*CDCA3*, *INCENP*, *OIP5*, and *RCC1*). Relative levels of endogenous Pygo2 mRNA (endo) were detected using primers that amplify the 3′ UTR of Pygo2. The graph represents qRT-PCR values that were normalized to both the control siRNA (siNTC) and empty pCS2 plasmid (EV).

Bar graphs represent averages ± SD. *p < 0.05; **p < 0.01; ***p < 0.001; ****p < 0.0001; NS, not significant. See also Figure S2 and Table S1. Error bars represent SD.

with centromeres in the normal perpendicular orientation, which was seen in cells transfected with the siNTC control. Similar results were obtained upon examination of the inner centromere protein (INCENP) (Figure S1E), which is essential for the capture of the mitotic spindle by the kinetochore during mitosis (Carmena et al., 2012). Overall, these observations suggested that depletion of Pygo2 caused inefficient chromosome capture.

Enrichment of Pygo2 at Transcriptional Start Sites of Genes Required for Cell Division

Since Pygo2 is excluded from mitotic chromatin (Andrews et al., 2013) and the expression of at least one candidate, AurKA, was affected by loss of Pygo2, we hypothesized that mitotic gene transcription is dependent on Pygo2. Chromatin immunoprecipitation sequencing (ChIP-seq) was, therefore, used to assess genome-wide association of Pygo2 with chromatin in HeLa S3 (S3) cells, since significant ChIP-seq *in silico* data exist for S3 cells from other chromatin studies. We found that 19% of peaks representing the most significant Pygo2 gene associations were within 3 kb of transcriptional start sites (TSSs), with Pygo2 enrichment occurring at promoter regions approximately 70 bp upstream (Figures 2A and 2B). Consistently, functional enrichment analysis of genes at TSSs using DAVID (Huang et al., 2009), revealed significant biological processes associated with cell cycle and mitosis (Figure 2C).

To corroborate the aforementioned *in silico* data, we depleted Pygo2 from S3 cells and performed RNA sequencing (RNA-seq). Comparison of differentially expressed genes using a control siRNA and two Pygo2-targeting siRNAs identified 287 upregulated and 92 downregulated genes (Figures S2A–S2D; Table S1). Gene ontology (GO) analysis revealed that upregulated genes were associated with cell proliferation and cell adhesion,

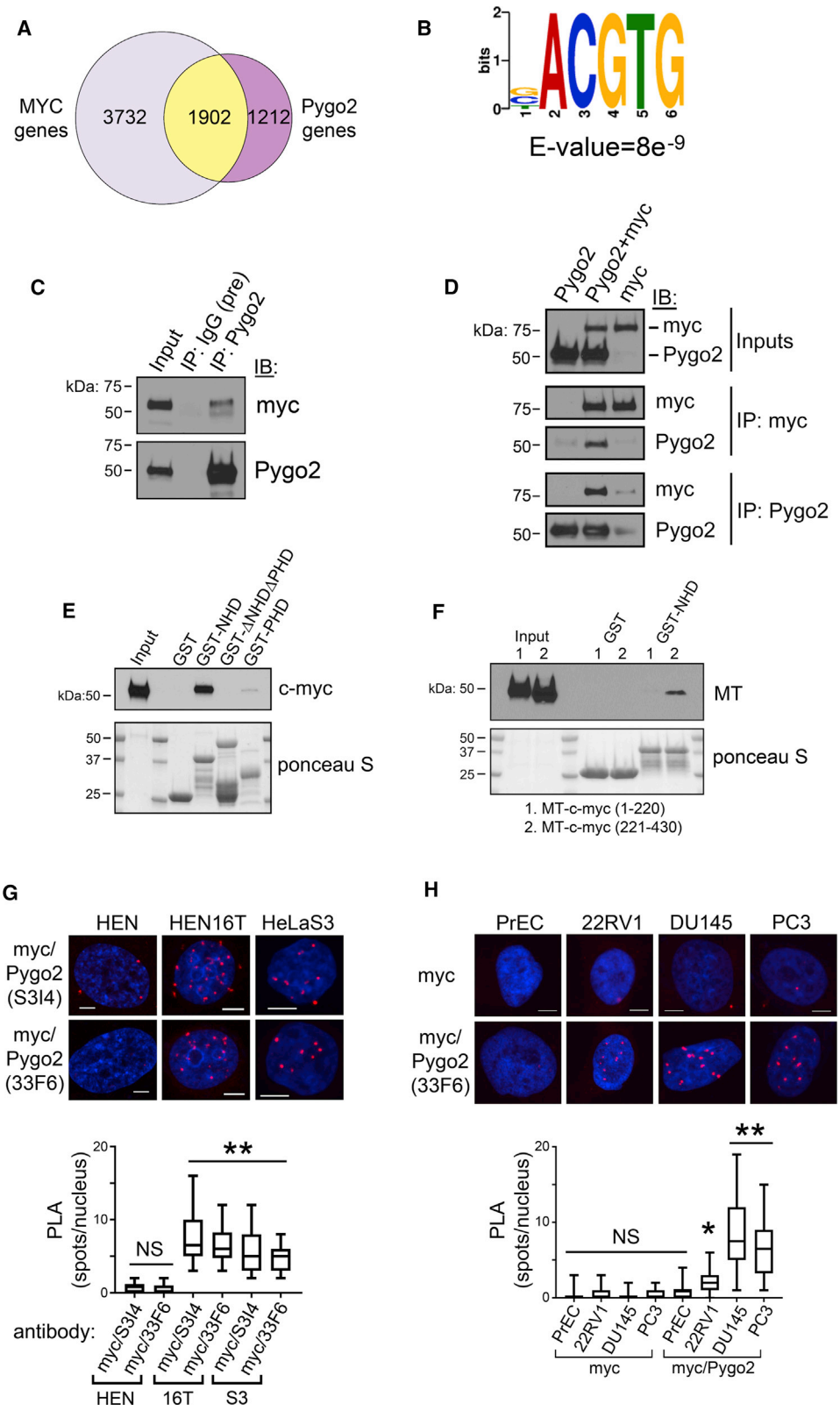

(legend on next page)

while downregulated ones were associated with mitosis and cell cycle (Figures S2E and S2F), consistent with ChIP-seq results. Notably, many of the genes that promote attachment between kinetochores and mitotic spindle microtubules (Katayama et al., 2008; Moore et al., 2002; Varma and Salmon, 2012) were sensitive to the loss of Pygo2 (Figure 2D), consistent with observed chromosome biorientation defects (Figure 1).

To confirm siRNA targeting specificity, Pygo2 was depleted in cells using an siRNA targeting the 3′ UTR of *pygo2* (siPy2-1) and rescued using a plasmid containing the Pygo2 wild-type (WT) coding region (Figure 2E). Expression of exogenous Pygo2 protein from this plasmid in the absence of endogenous Pygo2 mRNA resulted in the restoration of the expression of the mitotic genes *CDCA3*, *INCENP*, *OIP5*, and *RCC1* (Figure 2F). Thus, exogenously expressed Pygo2 mitigated the loss of endogenous Pygo2, confirming RNAi specificity.

We also assessed the role of the association of Pygo2 with H3K4me3 on Pygo2-responsive genes by co-expressing a H3K4me3 binding mutant of Pygo2 with the 3′ UTR targeting siRNA (Figure 2E, Y327A; Gu et al., 2009). While expression of most Pygo2-responsive genes could not be rescued with Pygo2 Y327A (Figure 2F), a minor but significant rescue of INCENP expression suggested that *INCENP* may not fully rely on Pygo2-H3K4me3 binding. Thus, Pygo2-H3K4me3 binding is important for expression of many, but not necessarily all, Pygo2-responsive genes.

Pygo2 Interacts with MYC in Cancer Cells

Several of the Pygo2 responsive genes such as *AurKA* and *RCC1* (Figure 2D), are established MYC targets (den Hollander et al., 2010; Tsuneoka et al., 1997); therefore, Pygo2 and MYC may associate to regulate similar sets of genes. ChIP-seq public-domain (encyclopedia of DNA elements [ENCODE]) data for MYC binding in S3 cells were compared with data obtained for Pygo2 to ascertain an *in silico* association. We identified an overlap of approximately 60% of Pygo2-enriched TSSs that were co-occupied by MYC (Figure 3A). Furthermore, motif enrichment analysis of chromatin-associated Pygo2 revealed the presence of MYC E-box binding motifs (Figure 3B).

Evidence for a physical interaction between Pygo2 with MYC was obtained by co-immunoprecipitation of exogenously expressed Pygo2 and MYC proteins in S3 cells (Figure 3C). This finding was corroborated in HEK293 cells co-transfected with Pygo2 and myc-tagged (MT) MYC, by performing forward and reverse immunoprecipitations (Figure 3D). Similarly, *in vitro* glutathione S-transferase (GST) pull-downs identified an interaction between the N-terminal homology domain (NHD) of Pygo2 and the C-terminal half of MYC (Figures 3E and 3F), containing the DNA binding and MAX dimerization domains (Blackwood and Eisenman, 1991).

Sub-cellular localization of exogenous, as well as endogenously expressed, proteins was visualized in the nuclei of S3 cells (Figures S3A–S3C). Elevation of MYC by overexpression or proteasome inhibitors such as MG132 caused nucleolar accumulation (Arabi et al., 2003). Similarly, MG132 increased co-localization in the S3 cells of both MYC and Pygo2 to nucleolar regions (Figure S3B) as demonstrated previously (Andrews et al., 2013; Arabi et al., 2005; Grandori et al., 2005), suggesting the accumulation of MYC/Pygo2 complexes at sites of rRNA transcription.

Pygo2 expression is essential for the growth of cervical (Tzenov et al., 2013) and prostate (Kao et al., 2017) cancer cell lines. Consistently, Pygo2 and MYC levels were elevated in nuclei of cervical and prostate cancer cells, as compared to that of normal epithelial cells (Figure S3C). Proximity ligation assays (PLAs), which demonstrate *in situ* protein interactions (Söderberg et al., 2006), identified a significant increase in nuclear MYC/Pygo2 interactions in cervical cancer cells (Figures 3G and 3H; HEN16T and HeLa S3), as compared to normal human endocervical (HEN) cells (Figure 3G). Similarly, we found significantly more interactions in prostatic primary tumor cells (22RV1) as compared to normal prostate epithelial cells (PrECs), but fewer than in metastatic prostate tumor cells (DU145 and PC3). The observations that Pygo2 and MYC interact most frequently in metastatic cell lines suggested that the MYC/Pygo2 interaction correlates with disease aggressiveness.

The Pygo2/MYC Interaction Is Distinct from Canonical Wnt Signaling

Many mitogenic pathways converge to amplify MYC expression in cancer, including canonical Wnt signaling (Dang, 2012). Pygo2 is a component of the active Wnt/β-catenin complex, which also activates *myc* transcription (Chen et al., 2010; Gu et al., 2012; Liu et al., 2013; Talla and Brembeck, 2016; Zhou et al., 2016). It is possible that in our Pygo2-depletion experiments, loss of MYC-dependent cell division proteins was indirectly due to

Figure 3. Pygo2 Interacts with MYC in Cancer Cells

(A) Comparison of MYC and Pygo2 binding within ±2 kb of TSSS, revealing approximately 60% overlap of genes associated with Pygo2 and MYC.

(B) DREME motif analysis of Pygo2-associated genes revealed the presence of E-box motifs.

(C) Pygo2 and MYC interact in HeLa S3 cells. Cells were co-transfected with Pygo2 and MYC, and immunoprecipitations were performed with either pre-immune sera or Pygo2 antisera. IgG, immunoglobulin G.

(D) Pygo2 and MYC interact in HEK293 cells that were co-transfected and immunoprecipitated (IP) with MT-myc and Pygo2. Immunoblots (IB) were performed with myc and Pygo2 antibodies.

(E) GST-pull-down analysis indicating MYC interaction with the N-homology domain (NHD) of Pygo2. Membranes were stained with Ponceau S to visualize GST proteins.

(F) GST-pull-down demonstrating interaction of the Pygo2 NHD with the C-terminal amino acids (aa) 221–430 of MYC.

(G) Pygo2 and MYC interact specifically in the nuclei of transformed cervical cells (16T and S3) relative to primary (HEN) cells using Pygo2 antisera (S3I4) and a Pygo2 rabbit monoclonal antibody (33F6) (**$p < 0.0001$; NS, not significant) revealed by proximity ligation assay (PLA).

(H) Pygo2 and MYC interact specifically in the nuclei of transformed prostate cells (22RV1, DU145 and PC3) relative to primary prostate epithelial (PrEC) cells. Scale bars, 5 μm. *$p < 0.05$; **$p < 0.0001$; NS; not significant. See also Figure S3.

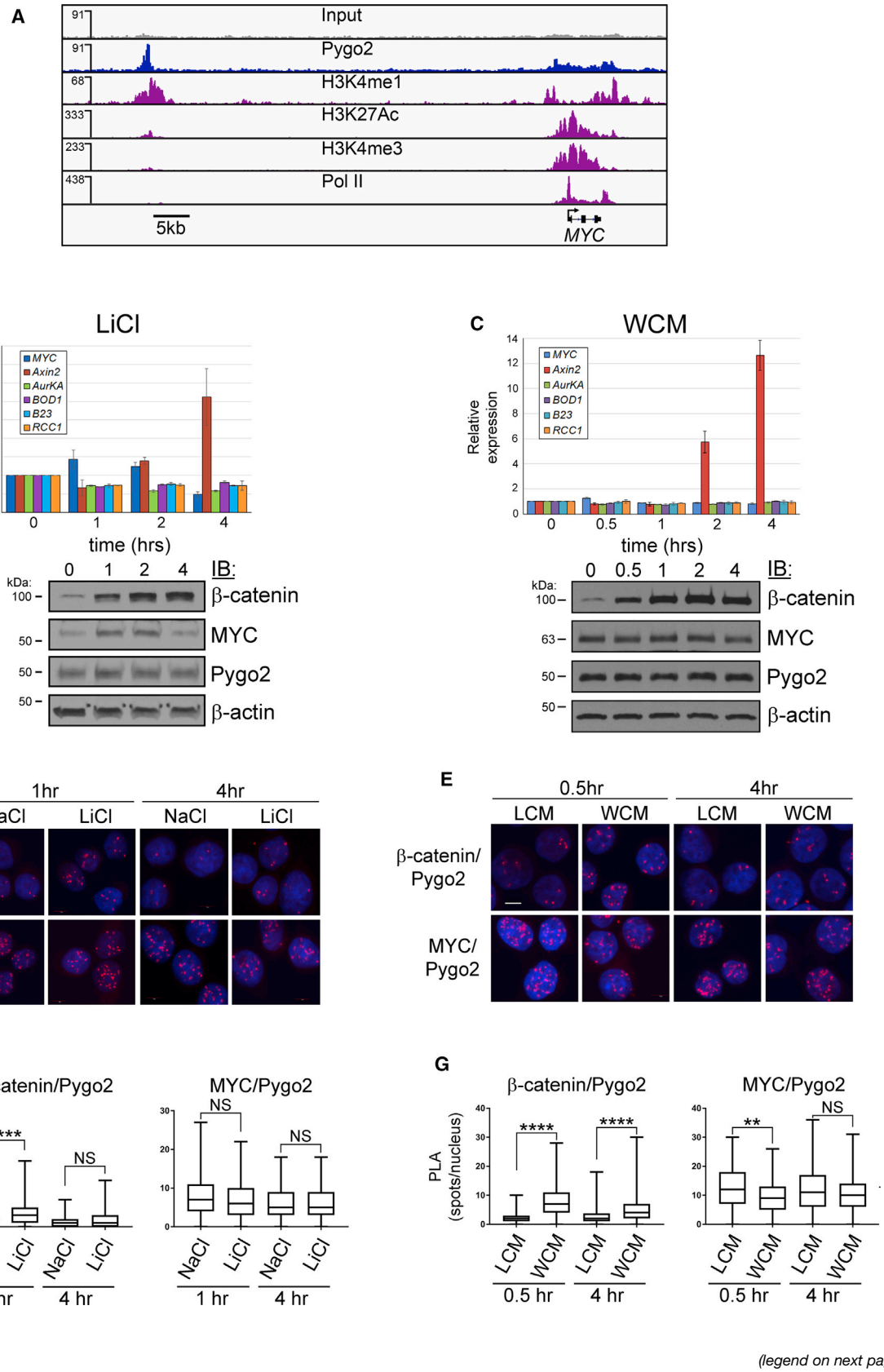

(legend on next page)

the attenuation of Wnt/β-catenin-mediated gene activation, including *myc* itself, rather than the interaction between Pygo2 and MYC. To investigate this possibility, we assessed the effect of Wnt signaling on mitotic gene expression and on the MYC/Pygo2 interaction.

Analysis of Pygo2 ChIP-seq data with public datasets for H3K4me1, H3K27Ac, H3K4me3, and RNA polymerase II (Pol II) confirmed Pygo2 association with upstream enhancer sequences of the *myc* gene in S3 cells, as expected (Figure 4A). To determine the effect of Wnt signaling on mitotic gene expression, we treated cells with LiCl (Klein and Melton, 1996) or Wnt3a conditioned media (WCM; Willert et al., 2003). Both LiCl and WCM resulted in a modest increase in MYC mRNA and protein expression at early time points (0.5 to 2 hrs Figures 4B and 4C). A robust increase in *AXIN2* mRNA was observed at later time points (2 to 4 hr; Figures 4B and 4C), confirming the ability of S3 cells to respond to Wnt signal transduction. The expression levels of *AURKA*, *BOD1*, *B23/NPM1*, and *RCC1* in response to Wnt/β-catenin activation were unchanged or modestly reduced (Figures 4B and 4C), indicating that MYC/Pygo2-dependent gene activation is not concomitant with Wnt signaling in S3 cells.

We next investigated the *in situ* association of Pygo2 with β-catenin or MYC in response to Wnt using PLAs (Figures 4D and 4E). Few β-catenin/Pygo2 associations were detected in the nuclei of both the unstimulated control NaCl or L-cell-conditioned-media (LCM)-treated cells (Figures 4D–4G). In the LiCl- and WCM-treated cells, there was a significant increase in the number of β-catenin/Pygo2 interactions detected at the early 1-hr and 0.5-hr time points, respectively (Figures 4F and 4G; $p < 0.0001$). At the 4-hr time point, significantly more β-catenin/Pygo2 nuclear interactions were detected in the WCM-treated cells (Figure 4G; $p < 0.0001$). Thus, Pygo2 associated with β-catenin within 1 hr in LiCl- and WCM-stimulated cells and for as much as 4 hr in WCM-treated cells, confirming the responsiveness of S3 cells to Wnt signaling.

MYC/Pygo2 interactions were largely equally abundant in all treated cells (Figures 4D–4G). A minor reduction was observed in the number of interactions at the early time points in both LiCl- and WCM-treated cells (Figures 4F and 4G), correlating with the reduction seen in MYC/Pygo2 target genes (Figures 4B and 4C). This observation suggested a transient shift in the pool of Pygo2 proteins to β-catenin-associated complexes from MYC complexes in response to Wnt signaling. Taken together, the aforementioned findings suggested that MYC/Pygo2 interactions and associated mitotic gene activity do not result from, and are likely independent of, *de novo* Wnt-induced Pygo2/β-catenin complexes.

Pygo2 Depletion Attenuates MYC-Dependent Transcription

Since Pygo2 was required for MYC expression (Figure 5A), we generated S3 cells that stably overexpressed MYC (S3/MYC), independent of endogenous *myc* expression, for Pygo2 loss-of-function studies. Pygo2 depletion in the S3 control line (S3/cont) reduced MYC expression but had no such effect on S3/MYC cells (Figures 5A and 5B). Moreover, there was an increase in p21 protein levels, which correlated with growth arrest in both the S3/cont and S3/MYC cells, indicating that MYC overexpression was not sufficient to rescue growth arrest caused by loss of Pygo2.

We next performed qRT-PCR in S3/cont and S3/MYC cells to examine the expression of common MYC target genes essential for cell growth (*47S, B23*, *CCNA1*, and *TERT*; Figure 5B) and cell division (*AurKA*, *BOD1*, *CEP290*, and *RCC1*; Figure 5B). Both MYC and Pygo2 were enriched at enhancer and promoter elements upstream of all the target genes analyzed (Figures 6A–6E; Figures S4B–S4D). Pygo2 knockdown attenuated the transcription of these genes, while rescue experiments demonstrated the specificity of siRNA knockdown and dependency on H3K4me3 binding (Figure S4A).

To investigate the role of Pygo2 in MYC-dependent transcription, we depleted Pygo2 in the S3/MYC cells (Figure 5C) and examined the binding of MYC and Pygo2 to promoter elements upstream of the *AurKA*, *BOD1*, and *RCC1* genes (Figure 5D). There was minimal change in the association of MYC with DNA, or with its E-box-specific binding partner MAX (Figure S4E). Conversely, depletion of MYC from S3 cells did not significantly affect overall Pygo2 protein levels (Figure 5E), nor did it reduce the association of Pygo2 with chromatin at *BOD1*, *AurkA*, and *RCC1* promoters (Figure 5F). Thus, Pygo2 and MYC associate with chromatin independently of each other.

Reduction of H3K27 Acetylation by Loss of Pygo2 at MYC-Associated Genes

Since Pygo2 and MYC bound independently to chromatin, the interaction between Pygo2 and MYC may be necessary to modify chromatin at promoters and/or enhancers for transcription. Enrichment of MYC and Pygo2 at common target genes strongly correlated with H3K27Ac enhancer/promoter peaks (Figures 6A–6E; Figures S4B–S4D). Thus, MYC/Pygo2 complexes promote or maintain H3K27Ac at actively transcribed genes.

Initially, we found that Pygo2 depletion had little effect on overall histone acetylation (Figure S5). A reduction of global H3K4me3 was observed, consistent with previous observations (Gu et al., 2009). When examined specifically at MYC/Pygo2-associated mitotic genes, H3K4me3, H3K9Ac, and H3K14Ac

Figure 4. MYC/Pygo2 Interaction Is Independent of Active Wnt/β-Catenin Signaling

(A) IGV genomic view of Pygo2 enrichment at *MYC* upstream enhancer sequences marked with H3K4me1 and H3K27Ac.

(B and C) Expression of Wnt target genes and MYC/Pygo2 target genes in HeLa S3 cells treated with 20 mM LiCl (B) or Wnt3a conditioned medium (WCM; C) at various time points (top panels) with representative immunoblots for β-catenin, MYC, and Pygo2 (bottom panels).

(D and E) Representative images obtained from PLAs examining the interaction between β-catenin/Pygo2 and MYC/Pygo2 in HeLa S3 cells treated with either 20 mM NaCl/LiCl (D) or L-conditioned medium (LCM)/WCM (E). Scale bars, 5 μm.

(F and G) Quantification of PLA spots observed per nucleus in cells treated with NaCl/LiCl (F) or LCM/WCM (G).

Bar graphs represent mean ± SD. **$p < 0.01$; ****$p < 0.0001$; NS, not significant.

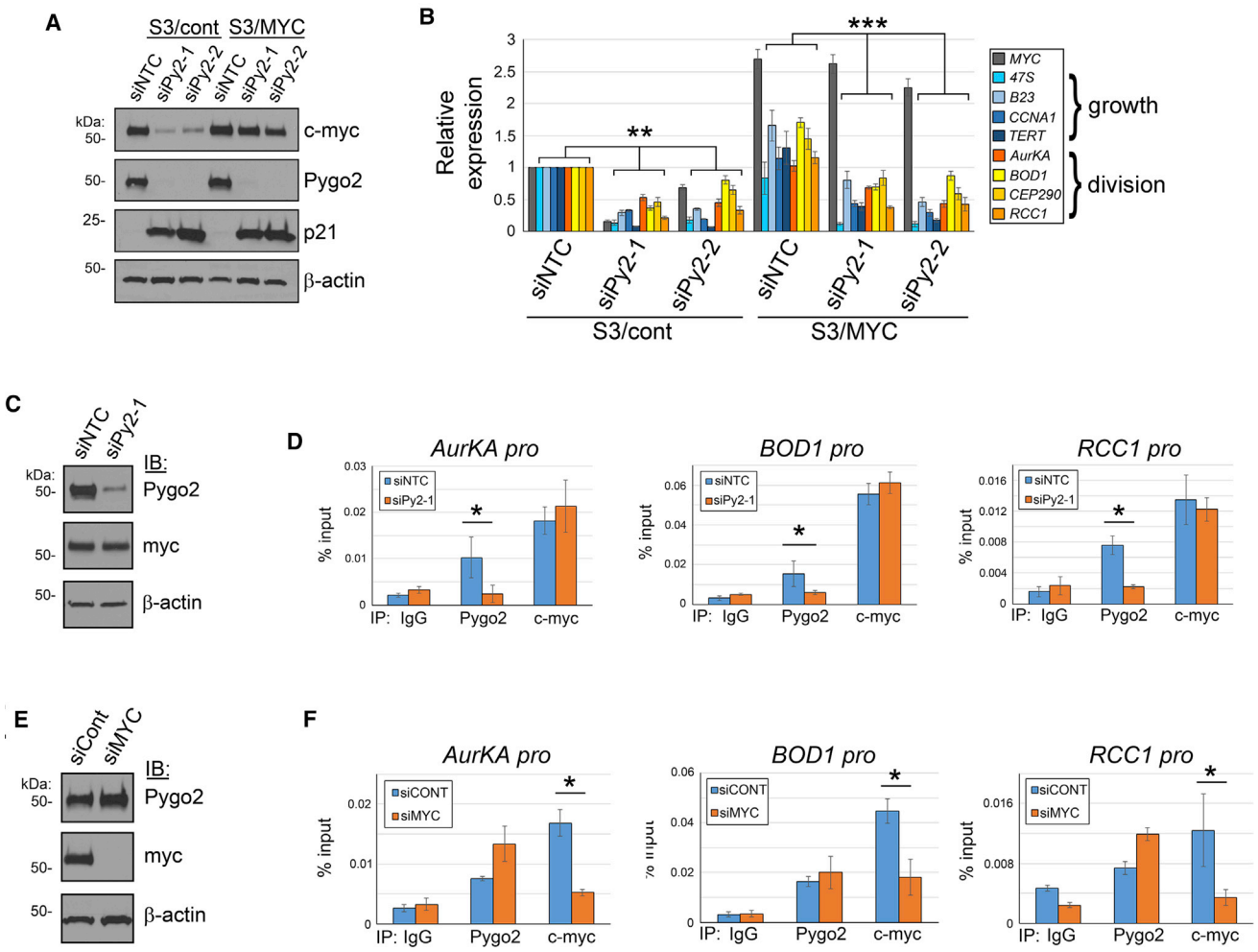

Figure 5. MYC-Regulated Transcription Depends on Pygo2

(A) Pygo2-dependent cell-cycle arrest and increase in p21 expression in control (S3/cont) and MYC (S3/MYC) cells.

(B) Depletion of Pygo2 in S3/cont and S3/MYC cells and expression analysis (qRT-PCR) of MYC target genes involved in cell growth and cell division.

(C and D) Depletion of Pygo2 in S3/MYC cells followed by immunoblotting for Pygo2 and MYC (C) and ChIP-qPCR to assess the binding of Pygo2 and MYC to the *AurKA*, *BOD1*, and *RCC1* promoters (D).

(E and F) Depletion of MYC in HeLa S3 cells, followed by immunoblotting for Pygo2 and MYC (E) and ChIP-qPCR to assess the relative binding of Pygo2 and MYC to the *AurKA*, *BOD1*, and *RCC1* promoters (F).

Bar graphs represent averages ± SEM. *$p < 0.05$; **$p < 0.01$; ***$p < 0.001$. See also Figure S4.

were unaffected, while H3K27Ac was significantly reduced (Figures 6F–6J), consistent with reductions in MYC target gene expression (Figures 2D and 5B). Thus, both Pygo2 and MYC may serve to maintain H3K27Ac at genes required for cell division.

Pygo2 in MYC-Driven Prostate Cancer Cells

In prostate cancer, *myc* rearrangements and deregulation of MYC mRNA and protein expression are important observations associated with tumor aggressiveness (Hawksworth et al., 2010). Similarly, elevated levels of Pygo2 in prostatectomy cancer specimens were associated with, or portended poorer prognosis (Kao et al., 2017). To assess the role of Pygo2 in MYC-driven cancer, we utilized the Myc-Cap cell line, derived from an advanced prostatic carcinoma of a mouse harboring a human c-*myc* transgene driven by an androgen-induced prostate epithelial-specific probasin promoter (ARR_2PB-myc; Ellwood-Yen et al., 2003; Watson et al., 2005).

Both MYC and Pygo2 proteins were elevated in mouse embryonic fibroblasts (MEFs) immortalized by simian virus 40 (SV-40), as compared to primary MEFs (Figure 7A). In Myc-Cap cells, both the *myc* transgene and *mPygo2* were both highly expressed (Figure 7A). Interaction of both endogenous mPygo2 and MYC protein in these cells was demonstrated, by immunoprecipitating mPygo2 from DNase-treated chromatin-bound fractions of Myc-Cap cells (Figure 7B), and by performing *in situ* PLAs (Figure 7C).

As in S3 cells, depletion of mPygo2 from Myc-Cap cells by RNAi did not affect MYC expression (Figures 7D and 7E) but reduced *AurKA* and *NPM1/B23* (Figure 7E) mRNA levels and

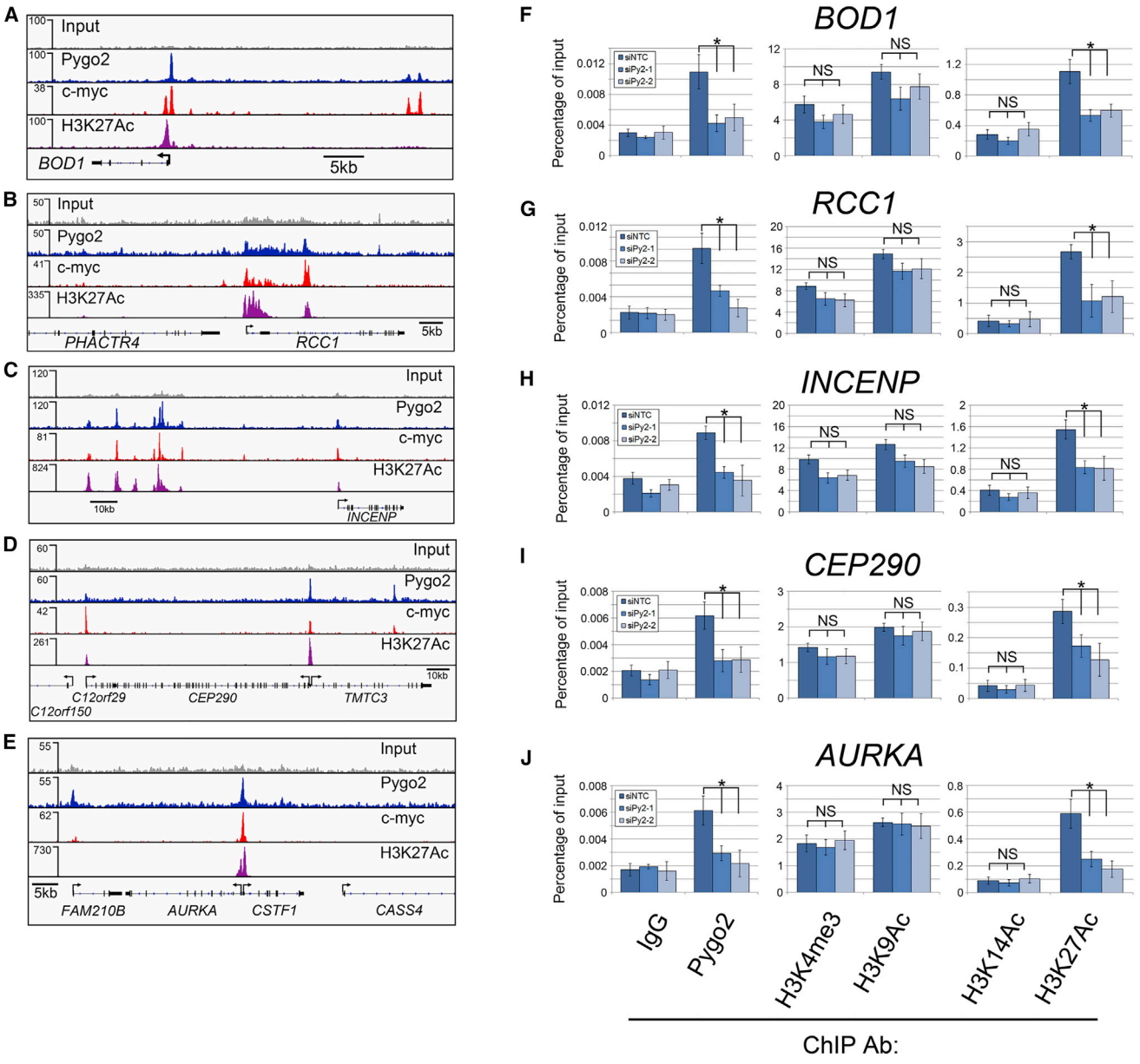

Figure 6. Pygo2 and MYC Are Co-enriched at Active Enhancers/Promoters Where Pygo2 Is Required for H3K27 Acetylation

(A–E) IGV genomic views of relative Pygo2, MYC, and H3K27Ac enrichment at sequences upstream of the mitotic target genes: BOD1 (A), RCC1 (B), INCENP (C), CEP290 (D), and AurkA (E).

(F–J) Examination of the relative enrichment of Pygo2, H3K4me3, H3K9Ac, H3K14Ac, and H3K27Ac in Pygo2-depleted HeLa S3 cells at the *BOD1* (F), *RCC1* (G), *INCENP* (H), *CEP290* (I), and *AurKA* (J) promoters.

Bar graphs represent averages ± SEM. *$p < 0.05$; NS, not significant. See also Figure S5.

attenuated growth and colony formation (Figures 7F and 7G) after 72 hr. These results indicated that Pygo2 interacts with MYC and plays an essential role in MYC-driven transcription and cell growth in a heterologous system.

DISCUSSION

Our findings suggest that a MYC/Pygo2-dependent transcriptional program is critical for microtubule-kinetochore interactions to facilitate chromosome biorientation during mitosis. For example, Pygo2 was required to maintain the expression and H3K27Ac levels within the vicinity of *AurKA*, *TPX2*, *RCC1*, *BOD1*, *CEP290*, and *INCENP* genes, which are needed for proper chromosome segregation and cell division. The chromosome alignment anomalies we found are similar to those found in cells deficient in Biorientation of Chromosomes in Division 1 (BOD1), a kinetochore protein required for the detection of syntelic attachments by the mitotic spindle (Porter et al., 2007). Our

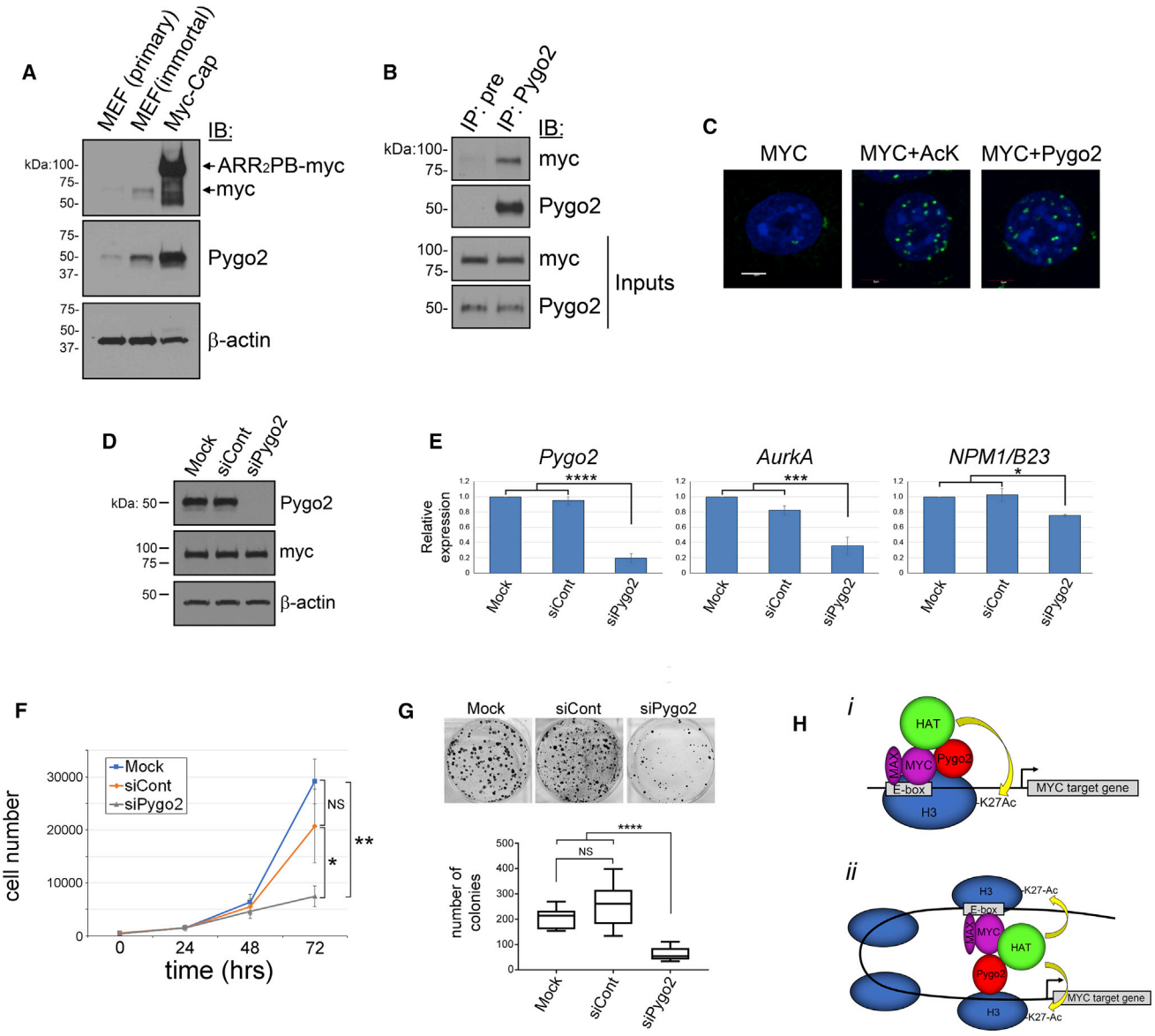

Figure 7. Pygo2 Interacts with MYC and Is Essential for Growth of a MYC-Driven Prostate Tumor Cell Model

(A) Immunoblot analysis of MYC and Pygo2 in primary and SV-40 immortalized MEFs and Myc-Cap cells.

(B) Immunoprecipitation of endogenous proteins using either preimmune serum (pre) or Pygo2 antiserum from chromatin bound fractions of Myc-Cap cells.

(C) Proximity ligation assays demonstrate *in situ* interaction between MYC and Pygo2 in nuclei of Myc-Cap cells. MYC antibodies and MYC/acetyl-lysine (AcK) were used as negative and positive controls, respectively. Scale bar, 5 μm.

(D) Knockdown of mPygo2 by RNAi in Myc-Cap cells followed by immunoblotting for Pygo2 and MYC. β-actin was used as a loading control.

(E) qRT-PCR analysis of Pygo2 along with MYC/Pygo2 target genes AurKA and NPM1/B23 in mPygo2-depleted Myc-Cap cells. Bar graphs represent means ± SD.

(F) Cell growth assay demonstrating reduction in cell numbers after 72 hr of siRNA treatment.

(G) Colony formation assay demonstrating reduction in colony number of cells treated with the mouse-specific Pygo2 siRNA.

(H) Proposed mechanism of the transcriptional control of cell division by Pygo2 and MYC in cancer cells. E-box bound MYC complexes and H3K4me3 bound Pygo2 complexes are suggested to promulgate H3K27 acetylation at enhancers/promoters of MYC target genes involved in oncogenic mitosis. MYC/Pygo2 complex formation may promote communication between DNA and histones (*i*) and/or interactions that encourage enhancer-promoter looping (*ii*), necessary for H3K27Ac.

*p < 0.05; **p < 0.01; ***p < 0.001; ****p < 0.0001; NS, not significant.

results are also consistent with overexpression of a mutant form of RCC1 (Moore et al., 2002). Pygo2-dependent RCC1 expression might, therefore, maintain a RanGTP concentration gradient necessary for microtubule nucleation and kinetochore recognition (Kalab and Heald, 2008). TPX2 and AurKA are key to the formation of kinetochore-derived microtubule nucleation that aids spindle-kinetochore interactions (Katayama et al., 2008). While we could not detect AurKA at kinetochores, the overall reduction of activated AurKA at centrosomes in Pygo2-deficient cells would account for decreased spindle-kinetochore interactions. Furthermore, CASC5/Knl-1, HAUS8, OIP5, and CKAP5 are all major constituents of the KMN network, required for the physical interaction between centromeric DNA and the spindle microtubules (Varma and Salmon, 2012).

In canonical Wnt signaling, Pygo2 binds via its plant homeodomain (PHD) to H3K4me3 in cooperation with Bcl9 (Fiedler et al., 2008), but whether this role is universal has been challenged (Cantù et al., 2013). In cancer cells, Pygo2-H3K4me3 binding is important for growth and expansion (Gu et al., 2009), and in the present study, most of the MYC/Pygo2 target genes were not activated by Pygo2 (Y327A) mutants (Figures 2F and S4A), substantiating the requirement for Pygo2-H3K4me3 binding. These observations support the idea that interactions between Pygo2 and MYC are consistent with the recruitment of HATs shared in common by both proteins, including: TRRAP, GCN5/PCAF, and CBP/p300, which are required for nucleosome remodeling. Thus, the MYC/Pygo2 interaction could be implicated in histone-DNA communication (Figure 7H*i*) or enhancer-promoter looping (Figure 7H*ii*), resulting in acetylation to H3K27 at upstream sequences of active target genes.

Active T-cell factor (TCF)/β-catenin complexes potentiate transcription of critical genes required to drive cell-cycle progression and growth, including *cyclin D1* and *myc* (He et al., 1998; Shtutman et al., 1999). While Pygo2 is a component of β-catenin complexes that promote cell-cycle entry, it appears to be recruited to MYC in complexes distinct from β-catenin once cells are committed to mitosis. In cancer, since MYC activity responds to multiple mitogenic pathways (Dang, 2012), the formation of MYC/Pygo2 complexes might also occur by alternate pathway activation apart from Wnt signaling. Thus, our results suggest that Pygo2 is an essential core component of the oncogenic MYC transcription complex.

EXPERIMENTAL PROCEDURES

Cell Lines and Antibodies

SKOV-3, HeLa S3 (S3), HEK293, 22RV1, DU145, PC3, and MYC-Cap cells were obtained from the American Type Tissue Collection (ATCC); primary HEN cells and transformed endocervical (HEN16T) cells (Tsutsumi et al., 1992) were provided by A. Pater. Primary PrECs (Lonza) were cultured in PrEBM medium by adding PrEGM single aliquots (Lonza), and primary HEN cells were cultured in DMEM supplemented with 2.1 μL/mL bovine pituitary extract and 0.06 μL/mL epidermal growth factor (EGF) (GIBCO). 22RV1 cells were cultured in RPMI 1640 media supplemented with 10% fetal bovine serum (FBS). All other cell lines were cultured in DMEM with 10% FBS. Stable clones expressing empty plasmid (S3/cont) or MYC (S3/MYC) were generated by transfecting pIRES-EGFP or pIRES2-EGFP-MYC into S3 cells. Isolated colonies were maintained in DMEM with 10% FBS and 200 μg/mL Geneticin (Invitrogen). Primary MEFs from E13.5 *pygo2*$^{f/f}$ embryos were immortalized by transfecting with pCMV-SV40 large T antigen (de Chasseval and de Villartay, 1992), selected by serial passaging and cultured in DMEM with 10% FBS.

Pygo2 rabbit monoclonal antibodies (33F6) were raised against amino acids 91–119 of Pygo2 (Immunoprecise). All other antibodies/antisera used are listed in the Supplemental Experimental Procedures.

RNAi, Plasmids, and Transfections

Non-targeting (siNTC) and Pygo2 (siPy2) siRNAs (for sequences, see the Supplemental Experimental Procedures) were used as described previously (Andrews et al., 2013). Control, MYC, and mouse-specific Pygo2 siRNA pools (Dharmacon) were transfected using Lipofectamine RNAiMAX (Invitrogen) at a final concentration of 5 nM. For rescue experiments, 5 nM siRNA was co-transfected with 500 ng of plasmids; protein and RNA were collected after 72 hr. For cell growth assays, 1,000 Myc-Cap cells were treated with siRNAs in 96-well plates. Cell number was determined using CellTiter 96 MTS Reagent (Promega). For colony formation assays, 500 Myc-Cap cells were treated with siRNAs for 72 hr in 6-well plates. Colonies were fixed in 10% neutral buffered formalin, stained with crystal violet, and counted. Results were obtained from 3 experiments performed in triplicate.

MYC sequences were amplified from primary HEN cells and inserted into pCS2+, pCS4-myc tag (MT), and pIRES2-EGFP. pCS2-Pygo2 Y327A was generated using the QuikChange Site-Directed Mutagenesis Kit (Agilent Technologies). pCS2+-Pygo2, GST-NHD, GST-ΔNHDΔPHD, and GST-PHD are described elsewhere (Andrews et al., 2009). Plasmids were transfected using Lipofectamine 2000 (Invitrogen).

Immunoblotting, Immunofluorescence, and PLAs

Immunoblotting and immunofluorescence (IF) were performed exactly as described previously (Andrews et al., 2013). IF was imaged under confocal microscopy (Olympus). Cell-counting assays were performed in triplicate for mitotic cells from 5 random fields per treatment and classified according to the observed mitotic profiles. PLAs were carried out on 4% paraformaldehyde (pH 7)-fixed cells using the Duolink PLA Kit (Sigma-Aldrich) and quantified either manually or by using BlobFinder software (Allalou and Wählby, 2009).

Immunoprecipitations and GST Pull-Downs

Cells were extracted in RIPA buffer (1.1% Triton X-100, 0.01% SDS, 1.2 mM EDTA, 16.7 mM Tris [pH 8.1], and 167 mM NaCl) supplemented with protease inhibitors (PIs) and PMSF. Immunoprecipitations and GST-pull-downs were performed using either HEK293 or S3 transfected cell extracts as previously described (Andrews et al., 2009). For chromatin-bound protein fractions, cells were lysed in RIPA buffer and sonicated for 1 min (10-s pulses with 30-s rests). $MgCl_2$ was added to a final concentration of 3 μM, and lysates were treated with 50 U of DNase I for 20 min at room temperature and cleared by centrifugation at 20,000 × *g* at 4°C before immunoprecipitation.

qRT-PCR and ChIP-qPCR

Total RNA, extracted using an RNeasy Kit (QIAGEN), was reverse transcribed using M-MLV Reverse Transcriptase (Invitrogen), as per the manufacturer. qRT-PCR analysis was performed using RT2 SYBRGreen Master Mix (QIAGEN) and oligonucleotide primers (for sequences, see the Supplemental Experimental Procedures). Relative values were calculated using the $2^{-\Delta\Delta Ct}$ method, normalized relative to β-actin expression. Chromatin DNA for ChIP was collected from formaldehyde-crosslinked cells by nuclear extraction in RIPA buffer supplemented with PIs and PMSF and sheared using a Sonic Dismembrator 100 (Fisher) to 300–500 bp. 1 mg chromatin was immunoprecipitated using 3 μg antibody and incubated with preblocked protein A beads (Millipore) to capture antibody-protein-DNA complexes. Beads were washed 3× in low-salt buffer (1.0% Triton X-100, 0.1% SDS, 2 mM EDTA, 20 mM Tris [pH 8.1], 150 mM NaCl), followed by 1× in high-salt buffer (1.0% Triton X-100, 0.1% SDS, 2 mM EDTA, 20 mM Tris [pH 8.1], 500 mM NaCl), followed by Tris-EDTA buffer. Complexes were eluted in elution buffer (1.0% SDS and 100 mM $NaHCO_3$); crosslinks were reversed at 65°C overnight. Samples were RNase A and proteinase K treated before purifying the DNA using the QIAquick PCR Purification Kit (QIAGEN). qPCR was performed using primers described in Table S1. Values were calculated relative to input controls. Results represent averages ± SEM from at least two independent experiments.

ChIP-Seq and Bioinformatics

ChIPs were performed as described earlier using Pygo2 S3I4 antisera (Tzenov et al., 2016) and 10^8 S3 cells. 20 ng of DNA was sequenced on an Illumina HiSeq 2500 sequencer (McGill University Genome Quebec Innovation Center). Reads were aligned to Hg19 using Burrows-Wheeler aligner-MEM (BWA-MEM). Downloaded ChIP-seq datasets performed in S3 cells from ENCODE included: input for MYC (ENCCFF390CZH), MYC (ENCHH000XCI), H3K4me1 (ENCSR000APW), H3K4me3 (ENCSR000AOF), RNA Pol II (ENCSR000EZL), and H3K27Ac (ENCSR000AOC). High confidence peaks were normalized against input and calculated using the Model-based Analysis for ChIP-Seq (MACS) peak caller (p value cutoff = 10^{-5}), with a false discovery rate < 1.2% (Zhang et al., 2008). Peaks with over 20-fold enrichment were used in downstream analyses. Motif enrichment analysis was performed using Discriminative Regular Expression Motif Elicitation (DREME; Machanick and Bailey, 2011), and annotation of peaks relative to genomic region was performed using the *cis*-Regulatory Element Annotation System (CEAS; Shin et al., 2009). Functional enrichment analysis and comparison of MYC/Pygo2 association with TSSs were performed using the Genomic Regions Enrichment of Annotations Tool (GREAT), v3.0.0 (McLean et al., 2010), and gene ontology of Pygo2 at TSSs was performed using the Database for Annotation, Visualization and Integrated Discovery (DAVID; Dennis et al., 2003). Pygo2 ChIP-seq analysis was independently confirmed using the ChIPseeker R/Bioconductor package (Yu et al., 2015).

Statistical Analysis

GraphPad Prism software was used to perform all statistical analyses, including one-way ANOVA along with Tukey's multiple comparison test to compare multiple treatment groups and Student's t test to compare two groups (α = 0.05). Experimental data (except for boxplots) were expressed as means ± SD or means ± SEM.

DATA AND SOFTWARE AVAILABILITY

The accession number for the aligned and normalized Pygo2 ChIP-seq data reported in this paper is GEO: GSE112291.

SUPPLEMENTAL INFORMATION

Supplemental Information includes Supplemental Experimental Procedures, five figures, and one table and can be found with this article online at https://doi.org/10.1016/j.celrep.2018.04.020.

ACKNOWLEDGMENTS

We thank Roya Derwish for helpful comments and suggestions. This research was funded by grants from the Canadian Institutes of Health Research (RNL135561), the Research and Development Corporation of NL (5404.1154.103), and The Motorcycle Ride for Dad (Avalon Chapter). This project was completed in partial fulfillment of the requirements for a doctoral degree for P.A.

AUTHOR CONTRIBUTIONS

P.G.P.A., K.R.K., and C.P. conceived the project. P.G.P.A. performed experiments. P.G.P.A. and K.R.K. analyzed data and wrote and edited the manuscript. T.J.B. helped with bioinformatic analysis, and C.P. edited the manuscript. K.R.K. and C.P. secured funding.

DECLARATION OF INTERESTS

K.R.K. and C.P. are co-inventors in U.S. Patent #007635560 – "Pygopus in diagnosis and treatment of cancer."

Received: February 23, 2016
Revised: September 14, 2017
Accepted: April 3, 2018
Published: May 1, 2018

REFERENCES

Allalou, A., and Wählby, C. (2009). BlobFinder, a tool for fluorescence microscopy image cytometry. Comput. Methods Programs Biomed. *94*, 58–65.

Andrews, P.G.P., Lake, B.B., Popadiuk, C., and Kao, K.R. (2007). Requirement of Pygopus 2 in breast cancer. Int. J. Oncol. *30*, 357–363.

Andrews, P.G.P., He, Z., Popadiuk, C., and Kao, K.R. (2009). The transcriptional activity of Pygopus is enhanced by its interaction with cAMP-response-element-binding protein (CREB)-binding protein. Biochem. J. *422*, 493–501.

Andrews, P.G.P., He, Z., Tzenov, Y.R., Popadiuk, C., and Kao, K.R. (2013). Evidence of a novel role for Pygopus in rRNA transcription. Biochem. J. *453*, 61–70.

Annibali, D., Whitfield, J.R., Favuzzi, E., Jauset, T., Serrano, E., Cuartas, I., Redondo-Campos, S., Folch, G., Gonzàlez-Juncà, A., Sodir, N.M., et al. (2014). Myc inhibition is effective against glioma and reveals a role for Myc in proficient mitosis. Nat. Commun. *5*, 4632.

Arabi, A., Rustum, C., Hallberg, E., and Wright, A.P.H. (2003). Accumulation of c-Myc and proteasomes at the nucleoli of cells containing elevated c-Myc protein levels. J. Cell Sci. *116*, 1707–1717.

Arabi, A., Wu, S., Ridderstråle, K., Bierhoff, H., Shiue, C., Fatyol, K., Fahlén, S., Hydbring, P., Söderberg, O., Grummt, I., et al. (2005). c-Myc associates with ribosomal DNA and activates RNA polymerase I transcription. Nat. Cell Biol. *7*, 303–310.

Archambault, V., Lépine, G., and Kachaner, D. (2015). Understanding the Polo Kinase machine. Oncogene *34*, 4799–4807.

Blackwood, E.M., and Eisenman, R.N. (1991). Max: a helix-loop-helix zipper protein that forms a sequence-specific DNA-binding complex with Myc. Science *251*, 1211–1217.

Cantù, C., Valenta, T., Hausmann, G., Vilain, N., Aguet, M., and Basler, K. (2013). The Pygo2-H3K4me2/3 interaction is dispensable for mouse development and Wnt signaling-dependent transcription. Development *140*, 2377–2386.

Carmena, M., Ruchaud, S., and Earnshaw, W.C. (2009). Making the Auroras glow: regulation of Aurora A and B kinase function by interacting proteins. Curr. Opin. Cell Biol. *21*, 796–805.

Carmena, M., Wheelock, M., Funabiki, H., and Earnshaw, W.C. (2012). The chromosomal passenger complex (CPC): from easy rider to the godfather of mitosis. Nat. Rev. Mol. Cell Biol. *13*, 789–803.

Chen, J., Luo, Q., Yuan, Y., Huang, X., Cai, W., Li, C., Wei, T., Zhang, L., Yang, M., Liu, Q., et al. (2010). Pygo2 associates with MLL2 histone methyltransferase and GCN5 histone acetyltransferase complexes to augment Wnt target gene expression and breast cancer stem-like cell expansion. Mol. Cell. Biol. *30*, 5621–5635.

Dang, C.V. (2012). MYC on the path to cancer. Cell *149*, 22–35.

Dang, C.V. (2013). MYC, metabolism, cell growth, and tumorigenesis. Cold Spring Harb. Perspect. Med. *3*, a014217.

Dang, C.V., Reddy, E.P., Shokat, K.M., and Soucek, L. (2017). Drugging the 'undruggable' cancer targets. Nat. Rev. Cancer *17*, 502–508.

de Chasseval, R., and de Villartay, J.P. (1992). High level transient gene expression in human lymphoid cells by SV40 large T antigen boost. Nucleic Acids Res. *20*, 245–250.

Degenhardt, Y., and Lampkin, T. (2010). Targeting Polo-like kinase in cancer therapy. Clin. Cancer Res. *16*, 384–389.

den Hollander, J., Rimpi, S., Doherty, J.R., Rudelius, M., Buck, A., Hoellein, A., Kremer, M., Graf, N., Scheerer, M., Hall, M.A., et al. (2010). Aurora kinases A and B are up-regulated by Myc and are essential for maintenance of the malignant state. Blood *116*, 1498–1505.

Dennis, G., Jr., Sherman, B.T., Hosack, D.A., Yang, J., Gao, W., Lane, H.C., and Lempicki, R.A. (2003). DAVID: database for annotation, visualization, and integrated discovery. Genome Biol. *4*, P3.

Ellwood-Yen, K., Graeber, T.G., Wongvipat, J., Iruela-Arispe, M.L., Zhang, J., Matusik, R., Thomas, G.V., and Sawyers, C.L. (2003). Myc-driven murine prostate cancer shares molecular features with human prostate tumors. Cancer Cell *4*, 223–238.

Fagnocchi, L., and Zippo, A. (2017). Multiple roles of MYC in integrating regulatory networks of pluripotent stem cells. Front. Cell Dev. Biol. *5*, 7.

Fiedler, M., Sánchez-Barrena, M.J., Nekrasov, M., Mieszczanek, J., Rybin, V., Müller, J., Evans, P., and Bienz, M. (2008). Decoding of methylated histone H3 tail by the Pygo-BCL9 Wnt signaling complex. Mol. Cell *30*, 507–518.

Foley, E.A., and Kapoor, T.M. (2013). Microtubule attachment and spindle assembly checkpoint signalling at the kinetochore. Nat. Rev. Mol. Cell Biol. *14*, 25–37.

Goldenson, B., and Crispino, J.D. (2015). The aurora kinases in cell cycle and leukemia. Oncogene *34*, 537–545.

Grandori, C., Gomez-Roman, N., Felton-Edkins, Z.A., Ngouenet, C., Galloway, D.A., Eisenman, R.N., and White, R.J. (2005). c-Myc binds to human ribosomal DNA and stimulates transcription of rRNA genes by RNA polymerase I. Nat. Cell Biol. *7*, 311–318.

Gu, B., Sun, P., Yuan, Y., Moraes, R.C., Li, A., Teng, A., Agrawal, A., Rhéaume, C., Bilanchone, V., Veltmaat, J.M., et al. (2009). Pygo2 expands mammary progenitor cells by facilitating histone H3 K4 methylation. J. Cell Biol. *185*, 811–826.

Gu, B., Watanabe, K., and Dai, X. (2012). Pygo2 regulates histone gene expression and H3 K56 acetylation in human mammary epithelial cells. Cell Cycle *11*, 79–87.

Hawksworth, D., Ravindranath, L., Chen, Y., Furusato, B., Sesterhenn, I.A., McLeod, D.G., Srivastava, S., and Petrovics, G. (2010). Overexpression of C-MYC oncogene in prostate cancer predicts biochemical recurrence. Prostate Cancer Prostatic Dis. *13*, 311–315.

He, T.C., Sparks, A.B., Rago, C., Hermeking, H., Zawel, L., da Costa, L.T., Morin, P.J., Vogelstein, B., Kinzler, K.W., Groden, J., et al. (1998). Identification of c-MYC as a target of the APC pathway. Science *281*, 1509–1512.

Huang, W., Sherman, B.T., and Lempicki, R.A. (2009). Bioinformatics enrichment tools: paths toward the comprehensive functional analysis of large gene lists. Nucleic Acids Res. *37*, 1–13.

Kalab, P., and Heald, R. (2008). The RanGTP gradient - a GPS for the mitotic spindle. J. Cell Sci. *121*, 1577–1586.

Kao, K.R., Popadiuk, P., Thoms, J., Aoki, S., Anwar, S., Fitzgerald, E., Andrews, P., Voisey, K., Gai, L., Challa, S., et al. (2017). PYGOPUS2 expression in prostatic adenocarcinoma is a potential risk stratification marker for PSA progression following radical prostatectomy. J. Clin. Pathol. Published September 18, 2017. https://doi.org/10.1136/jclinpath-2017-204718.

Katayama, H., Sasai, K., Kloc, M., Brinkley, B.R., and Sen, S. (2008). Aurora kinase-A regulates kinetochore/chromatin associated microtubule assembly in human cells. Cell Cycle *7*, 2691–2704.

Klein, P.S., and Melton, D.A. (1996). A molecular mechanism for the effect of lithium on development. Proc. Natl. Acad. Sci. USA *93*, 8455–8459.

Kollman, J.M., Merdes, A., Mourey, L., and Agard, D.A. (2011). Microtubule nucleation by γ-tubulin complexes. Nat. Rev. Mol. Cell Biol. *12*, 709–721.

Kramps, T., Peter, O., Brunner, E., Nellen, D., Froesch, B., Chatterjee, S., Murone, M., Züllig, S., and Basler, K. (2002). Wnt/wingless signaling requires BCL9/legless-mediated recruitment of pygopus to the nuclear beta-catenin-TCF complex. Cell *109*, 47–60.

Lin, C.Y., Lovén, J., Rahl, P.B., Paranal, R.M., Burge, C.B., Bradner, J.E., Lee, T.I., and Young, R.A. (2012). Transcriptional amplification in tumor cells with elevated c-Myc. Cell *151*, 56–67.

Liu, Y., Dong, Q.-Z., Wang, S., Fang, C.-Q., Miao, Y., Wang, L., Li, M.-Z., and Wang, E.-H. (2013). Abnormal expression of Pygopus 2 correlates with a malignant phenotype in human lung cancer. BMC Cancer *13*, 346.

Machanick, P., and Bailey, T.L. (2011). MEME-ChIP: motif analysis of large DNA datasets. Bioinformatics *27*, 1696–1697.

McLean, C.Y., Bristor, D., Hiller, M., Clarke, S.L., Schaar, B.T., Lowe, C.B., Wenger, A.M., and Bejerano, G. (2010). GREAT improves functional interpretation of *cis*-regulatory regions. Nat. Biotechnol. *28*, 495–501.

Meyer, N., and Penn, L.Z. (2008). Reflecting on 25 years with MYC. Nat. Rev. Cancer *8*, 976–990.

Moore, W., Zhang, C., and Clarke, P.R. (2002). Targeting of RCC1 to chromosomes is required for proper mitotic spindle assembly in human cells. Curr. Biol. *12*, 1442–1447.

Nie, Z., Hu, G., Wei, G., Cui, K., Yamane, A., Resch, W., Wang, R., Green, D.R., Tessarollo, L., Casellas, R., et al. (2012). c-Myc is a universal amplifier of expressed genes in lymphocytes and embryonic stem cells. Cell *151*, 68–79.

Parker, D.S., Jemison, J., and Cadigan, K.M. (2002). Pygopus, a nuclear PHD-finger protein required for Wingless signaling in *Drosophila*. Development *129*, 2565–2576.

Popadiuk, C.M., Xiong, J., Wells, M.G., Andrews, P.G., Dankwa, K., Hirasawa, K., Lake, B.B., and Kao, K.R. (2006). Antisense suppression of pygopus2 results in growth arrest of epithelial ovarian cancer. Clin. Cancer Res. *12*, 2216–2223.

Porter, I.M., McClelland, S.E., Khoudoli, G.A., Hunter, C.J., Andersen, J.S., McAinsh, A.D., Blow, J.J., and Swedlow, J.R. (2007). Bod1, a novel kinetochore protein required for chromosome biorientation. J. Cell Biol. *179*, 187–197.

Schwab, K.R., Patterson, L.T., Hartman, H.A., Song, N., Lang, R.A., Lin, X., and Potter, S.S. (2007). Pygo1 and Pygo2 roles in Wnt signaling in mammalian kidney development. BMC Biol. *5*, 15.

Shin, H., Liu, T., Manrai, A.K., and Liu, X.S. (2009). CEAS: *cis*-regulatory element annotation system. Bioinformatics *25*, 2605–2606.

Shtutman, M., Zhurinsky, J., Simcha, I., Albanese, C., D'Amico, M., Pestell, R., and Ben-Ze'ev, A. (1999). The cyclin D1 gene is a target of the beta-catenin/LEF-1 pathway. Proc. Natl. Acad. Sci. USA *96*, 5522–5527.

Söderberg, O., Gullberg, M., Jarvius, M., Ridderstråle, K., Leuchowius, K.J., Jarvius, J., Wester, K., Hydbring, P., Bahram, F., Larsson, L.G., and Landegren, U. (2006). Direct observation of individual endogenous protein complexes in situ by proximity ligation. Nat. Methods *3*, 995–1000.

Talla, S.B., and Brembeck, F.H. (2016). The role of Pygo2 for Wnt/ß-catenin signaling activity during intestinal tumor initiation and progression. Oncotarget *7*, 80612–80632.

Tanaka, T.U. (2010). Kinetochore-microtubule interactions: steps towards bi-orientation. EMBO J. *29*, 4070–4082.

Tanaka, K. (2013). Regulatory mechanisms of kinetochore-microtubule interaction in mitosis. Cell. Mol. Life Sci. *70*, 559–579.

Tanenbaum, M.E., and Medema, R.H. (2010). Mechanisms of centrosome separation and bipolar spindle assembly. Dev. Cell *19*, 797–806.

Thompson, B., Townsley, F., Rosin-Arbesfeld, R., Musisi, H., and Bienz, M. (2002). A new nuclear component of the Wnt signalling pathway. Nat. Cell Biol. *4*, 367–373.

Topham, C., Tighe, A., Ly, P., Bennett, A., Sloss, O., Nelson, L., Ridgway, R.A., Huels, D., Littler, S., Schandl, C., et al. (2015). MYC is a major determinant of mitotic cell fate. Cancer Cell *28*, 129–140.

Tsuneoka, M., Nakano, F., Ohgusu, H., and Mekada, E. (1997). c-*myc* activates RCC1 gene expression through E-box elements. Oncogene *14*, 2301–2311.

Tsutsumi, K., Belaguli, N., Qi, S., Michalak, T.I., Gulliver, W.P., Pater, A., and Pater, M.M. (1992). Human papillomavirus 16 DNA immortalizes two types of normal human epithelial cells of the uterine cervix. Am. J. Pathol. *140*, 255–261.

Tzenov, Y.R., Andrews, P.G., Voisey, K., Popadiuk, P., Xiong, J., Popadiuk, C., and Kao, K.R. (2013). Human papilloma virus (HPV) E7-mediated attenuation of retinoblastoma (Rb) induces hPygopus2 expression via Elf-1 in cervical cancer. Mol. Cancer Res. *11*, 19–30.

Tzenov, Y.R., Andrews, P., Voisey, K., Gai, L., Carter, B., Whelan, K., Popadiuk, C., and Kao, K.R. (2016). Selective estrogen receptor modulators and betulinic acid act synergistically to target ERα and SP1 transcription factor dependent Pygopus expression in breast cancer. J. Clin. Pathol. *69*, 518–526.

Varma, D., and Salmon, E.D. (2012). The KMN protein network–chief conductors of the kinetochore orchestra. J. Cell Sci. *125*, 5927–5936.

Watanabe, K., Fallahi, M., and Dai, X. (2014). Chromatin effector Pygo2 regulates mammary tumor initiation and heterogeneity in MMTV-Wnt1 mice. Oncogene *33*, 632–642.

Watson, P.A., Ellwood-Yen, K., King, J.C., Wongvipat, J., Lebeau, M.M., and Sawyers, C.L. (2005). Context-dependent hormone-refractory progression revealed through characterization of a novel murine prostate cancer cell line. Cancer Res. *65*, 11565–11571.

Whitfield, J.R., Beaulieu, M.E., and Soucek, L. (2017). Strategies to inhibit Myc and their clinical applicability. Front. Cell Dev. Biol. *5*, 10.

Willert, K., Brown, J.D., Danenberg, E., Duncan, A.W., Weissman, I.L., Reya, T., Yates, J.R., 3rd, and Nusse, R. (2003). Wnt proteins are lipid-modified and can act as stem cell growth factors. Nature *423*, 448–452.

Yu, G., Wang, L.G., and He, Q.Y. (2015). ChIPseeker: an R/Bioconductor package for ChIP peak annotation, comparison and visualization. Bioinformatics *31*, 2382–2383.

Zhang, Y., Liu, T., Meyer, C.A., Eeckhoute, J., Johnson, D.S., Bernstein, B.E., Nusbaum, C., Myers, R.M., Brown, M., Li, W., and Liu, X.S. (2008). Model-based analysis of ChIP-Seq (MACS). Genome Biol. *9*, R137.

Zhang, S., Li, J., He, F., and Wang, X.-M. (2015). Abnormal nuclear expression of Pygopus-2 in human primary hepatocellular carcinoma correlates with a poor prognosis. Histopathology *67*, 176–184.

Zhou, C., Zhang, Y., Dai, J., Zhou, M., Liu, M., Wang, Y., Chen, X.Z., and Tang, J. (2016). Pygo2 functions as a prognostic factor for glioma due to its up- regulation of H3K4me3 and promotion of MLL1/MLL2 complex recruitment. Sci. Rep. *6*, 22066.